Pakistan Veterinary Journal

ISSN: 0253-8318 (PRINT), 2074-7764 (ONLINE)
DOI: 10.29261/pakvetj/2026.068

RESEARCH ARTICLE

IL-1β/MMP-7/LOXL2/COL2A1 Mediates the Pathological Damage of the Metatarsophalangeal Articular Cartilage-Subchondral Bone in Ostrich Leg and Toe Disease

Yiyun Deng, Bowen Duan, Li Tang*, Ronghui Wang, Jiale Wang, Zhengli Chen, Jing Fang, Chao Huang, Wentao Liu, Qihui Luo, Lanlan Jia, Yi Geng, Ping OuYang, Hongrui Guo and Huidan Deng

[1]Department of Basic Veterinary Medicine, College of Veterinary Medicine, Sichuan Agricultural University, Chengdu 611134, P.R. China
*Corresponding author: tangli202511@163.com; tangyimingtt@163.com

ARTICLE HISTORY (25-542)

Received: June 10, 2025
Revised: March 14, 2026
Accepted: March 16, 2026
Published online: March 19, 2026

Key words:
Histopathology
IL-1β/MMP-7/LOXL2/COL2A1
Metatarsophalangeal joint
Ostrich leg and toe disease

ABSTRACT

Ostrich leg and toe disease causes substantial morbidity and economic losses; however, its etiology and pathological progression remain poorly understood and inadequately controlled. This study aimed to investigate pathological changes in the cartilage and subchondral bone of the metatarsophalangeal joint in ostriches with leg and toe disease, with particular emphasis on the expression of key inflammatory mediators. Eighteen 30-day-old male ostriches were divided into three groups (n=6 each): H (healthy), D1 (mild disease), and D2 (severe disease). Pathological changes were evaluated using hematoxylin–eosin (HE) and Masson's trichrome staining. The expression of IL-1β, MMP-7, LOXL2, and COL2A1 was analyzed at the mRNA level by quantitative reverse-transcription PCR (qRT-PCR) and at the protein level by immunofluorescence (IF) and enzyme-linked immunosorbent assay (ELISA). Joint effusion volume and metatarsophalangeal circumference were also measured. Compared with the H group, the D1 and D2 groups showed significant increases in joint fluid volume (D1 vs H, $P<0.01$; D2 vs D1, $P<0.01$) and joint circumference (D1 vs H, $P<0.01$; D2 vs D1, $P<0.05$). Histological examination revealed fragmentation of collagen fibers in the superficial cartilage, a reduction in chondrocytes in the middle layer, and loosely arranged trabeculae in the subchondral bone. IL-1β and MMP-7 were progressively upregulated at both mRNA and protein levels with increasing lesion severity (IL-1β: $P<0.01$; MMP-7: $P<0.01$). In contrast, LOXL2 and COL2A1 were progressively downregulated (LOXL2: $P<0.01$; COL2A1: D1 vs H, $P<0.01$; D2 vs D1, $P<0.05$). These findings demonstrate that the progressive upregulation of IL-1β and MMP-7, together with the downregulation of LOXL2 and COL2A1, is closely associated with lesion severity, suggesting that these mediators may play key roles in the pathogenesis of ostrich leg and toe disease and may serve as potential targets for therapeutic intervention.

To Cite This Article: Deng Y, Duan B, Tang L, Wang R, Wang J, Chen Z, Fang J, Huang C, Liu W, Luo Q, Jia L, Geng Y, OuYang P, Guo H and Deng H, 2026. IL-1β/MMP-7/LOXL2/COL2A1 mediates the pathological damage of the metatarsophalangeal articular cartilage-subchondral bone in ostrich leg and toe disease. Pak Vet J, 46(4): 920-929. http://dx.doi.org/10.29261/pakvetj/2026.068

INTRODUCTION

The African ostrich (*Struthio camelus*), an herbivore valued for its high economic return, is increasingly farmed worldwide (Umar, 2021). However, ostrich leg and toe disease remains a devastating threat to the industry: its incidence rate has been reported near 35%, and its elimination plus mortality rate has been reported to exceed 90% (Tang *et al*., 2012), with recent studies confirming it as a top cause of ostrich loss in intensive farming systems globally (Mushi *et al*., 2023). Lesions primarily occur during the brooding period (1-90 days of age) (Arend *et al*., 2008; Deng *et al*., 2016). Early-stage disease manifests as joint swelling, lameness, and, in severe cases, inability to bear weight (Sengupta *et al*., 2011); late-stage disease leads to death (Liu and Tang, 2001). Etiology remains complex and multifactorial (e.g., nutritional imbalance, mechanical overload, infection) (Wang, 2008; Zeng, 2019; Yuan *et al*., 2020; Peel *et al*., 2022), with no definitive consensus or effective prevention/treatment. Our previous work identified marked enlargement and effusion of the metatarsophalangeal joint in 30-day-old males, with

osteoarthritis-like histopathology (Duan, 2023). This similarity is not coincidental: avian long-legged species like ostriches share conserved joint pathophysiology with mammals where osteoarthritis (OA) is characterized by chondrocyte death, extracellular matrix (ECM) degradation, and aberrant subchondral bone osteoblast activity driving cartilage erosion and sclerosis (Lories and Luyten, 2011; Chiba *et al*., 2012; Hamann *et al*., 2013; Goldring and Goldring, 2016; Reina *et al*., 2017). Key inflammatory and matrix-related factors IL-1β, MMP-7, LOXL2, and COL2A1are critical regulators of this degenerative cascade in mammalian OA, justifying their focus here. Related inflammatory factors (IL-1β, MMP-7, LOXL2, and COL2A1) regulate these processes: IL-1β acts as a central proinflammatory cytokine and its upregulation promotes matrix metalloproteinase (MMP) expression and type II collagen (COL2) degradation (Roy *et al*., 2006; Sengupta *et al*., 2011). Moreover, MMP-7, a matrix metalloproteinase, directly degrades ECM components including proteoglycans and collagens (Neuhold *et al*., 2001; Zhou *et al*., 2023)LOXL2 exerts anabolic effects by enhancing COL2A1 synthesis, while its expression is suppressed by IL-1β (Lohmander *et al*., 2014; Alshenibr *et al*., 2017) COL2A1 encodes type II collagen, the primary structural component of articular cartilage whose loss is a hallmark of joint degeneration (Park *et al*., 2016; Mao *et al*., 2019)Therefore, we hypothesized that IL-1β/MMP-7 upregulation and LOXL2/COL2A1 downregulation mediate joint degeneration in diseased ostriches. We examined 30-day-old male ostriches and employed a combination of methods: clinical observation, HE staining, Masson staining, qRT-PCR, IF staining, and ELISA. Specifically, these approaches were used to characterize the pathological features of metatarsophalangeal articular cartilage-subchondral bone in ostrich leg and toe disease, as well as to track changes in the expression of related inflammatory factors.

Our primary aim was to determine whether these inflammatory factors are involved in the onset and progression of the disease. Additionally, this work sought to further explore the etiology and pathogenesis of the disease, with the ultimate goal of providing a theoretical basis for its prevention and treatment.

MATERIALS AND METHODS

Animals: Eighteen 30-day-old male African ostriches were sourced from Sanmu ostrich breeding farm in Mianyang City, Sichuan Province, acclimatized under uniform environmental conditions prior to sampling, and allocated into three groups (n=6 each): H (healthy), D1 (mild disease), D2 (severe disease), with all procedures complying with local animal welfare regulations. Inclusion criteria for diseased groups included manifestation of depression and reduced feed intake (A), tarsal joint swelling and lameness (B), and inability to stand (C, restricted to Group D2), while the exclusion criterion was the absence of other joint disorders such as infection, bone tumor, and fracture (D); specifically, Group D1 fulfilled criteria A, B, and D, Group D2 met all criteria A-D, and Group H showed no clinical signs of leg and toe disease and met exclusion criterion D.

Sample collection and histopathological analysis: The experimental procedure was reviewed and approved by the Animal Care and Use Committee of Sichuan Agricultural University (SYXK 2019-187). The circumference of the metatarsophalangeal joint with a tape was measured and recorded. Use a disposable syringe to draw the joint fluid of the ostrich metatarsophalangeal joint and inject it into a graduated cylinder to measure the total amount of joint fluid. Ostriches were first anesthetized with 20% urethane (via cervical vein), and loss of consciousness was confirmed prior to exsanguination via the carotid artery; the metatarsophalangeal joint was then exposed for subsequent procedures. The articular cartilage tissue was cut into pieces, and some of them were transferred to a low-temperature freezer at −80°C for storage. After being fixed in 4% paraformaldehyde solution for 24 hours, the samples were then placed in 10% EDTA solution for decalcification. The decalcification solution bottle was shaken to accelerate the decalcification process, and the decalcification solution was replaced every 3 days until all the calcium in the joints was removed (the decalcification endpoint was determined by no resistance when the needle was inserted). The decalcified tissues were washed with distilled water and then placed in 4% paraformaldehyde solution for storage and future use. Paraffin-embedded: Tissues were cut into 2mm pieces, placed in tissue embedding frames, and rinsed for 24 hours. Subsequently, samples were sequentially dehydrated in 75, 85, 95, 100 I, and 100% II ethanol with durations of 720, 720, 120, 30, and 30minutes, respectively. After clearing in xylene, tissues were infiltrated with paraffin at 60°C for 2hours, embedded, sectioned at 5μm, and dried for 24 hours. Sections were stained with Hematoxylin and Eosin (H&E) and Masson's trichrome stain (Wuhan Seville BioTech).

Quantitative histomorphometry: Ten tissue sections were randomly selected from each group. For each section, 15 fields of view were randomly selected for photography under an optical microscope with a magnification of 400×. The trabecular thickness and trabecular spacing of the subchondral bone in the photos were measured and statistically analyzed using the Image Pro Plus 6.0 measurement software (Media Cybernetics, Rockville, MD, USA). Chondrocytes, osteoblasts and cartilage lacuna vacancy rate were counted respectively under the same field of view area. Among them, the cartilage lacuna vacancy rate = vacant cartilage depressions/total cartilage depressions.

Quantitative characterization of disease severity: We used modified Mankin's score (Cheng *et al*., 2022; Miao *et al*., 2024) to verify whether the clinical symptom grouping was in line with the actual lesion degree of articular cartilage in Table 1.

Detection of inflammatory factors in the cartilage-subchondral bone of the metatarsophalangeal joint: To determine whether the related inflammatory factors IL-1β, MMP-7, LOXL2, and COL2A1 are involved in the lesions of the metatarsophalangeal joint cartilage-subchondral bone, we used qRT-PCR, IF and ELISA to verify their localization and expression at mRNA and protein levels.

qRT-PCR: Total RNA was extracted using TRIzol and reverse-transcribed to cDNA. qRT-PCR was conducted with SYBR Green (NovoStart®), GAPDH as the reference gene. Primer sequences are listed in Table 2.

Table 1: Modified Mankin scoring criteria for ostrich metatarsophalangeal cartilage (Miao *et al*., 2024)).

Cartilage structure	Score	Chondrocytes	Score	Matrix staining	Score	Integrity of the tidal line	Score
Light as usual	0	The quantity is as usual	0	normal	0	complete	0
Surface destruction	1	Diffuse increase	1	Mild loss of staining	1	Multiple tidal lines	1
Destruction of blood vessels and superficial layers	2	A large number of cluster-like cell clumps appear	2	Moderate staining	2	Subchondral vascular invasion of tidal lines	2
Shallow fissures form up to the migratory layer	3	The number has decreased significantly	3	Severe loss of staining	3		
The fissure reaches as deep as the radiation layer	4			The staining disappears completely	4		
The fissure reaches deep into the calcified layer	5						
Complete destruction of the structure	6						

Table 2: Primer sequence

Primer name	Primer sequence (5'-3')	Tm (°C) (F/R)	Amplicon size (bp)	NCBI Accession
IL-1β	F : AGGCCCGGCCCGAAGCGGCG	68.5 / 67.8	212	XM_009682937.3
	R : TGCTTGGGCTGCCGCGAGGG			
MMP-7	F : CCTTGTTGCTGCTCACGAATTTGG	59.2 / 60.1	184	XM_009678588.3
	R : AAAGCCGGAAGGTTTTGGGGTTC			
LOXL2	F : TGCCATCCTCGCCACCTACC	62.4 / 63.0	241	XM_009688520.3
	R : ATCCAAACATGCCACAGACGACTC			
COL2A1	F : CTGCCACTGCTTGCCACTCTAC	61.8 / 62.5	193	XM_009680834.3
	R : AGCCTCACATCGGAAGGAGACAG			
GAPDH	F : GGTAGTGAAGGCTGCTGCTG	59.5 / 60.2	132	XM_009685444.3
	R : AGCACCTGCATCAAAGGTGG			

Immunofluorescence studies (IF): Paraffin sections were taken for antigen repair, then rinsed with phosphate-buffered saline (PBS). BSA was dropped and placed in a wet box for sealing for 30minutes. For negative control groups, PBS was used to replace the primary antibodies (no primary antibody added), and all other experimental procedures (including blocking, incubation conditions, secondary antibody incubation, and washing steps) were performed in parallel and kept consistent with the experimental groups. For experimental groups, primary antibodies IL-1β, MMP-7, LOXL2, and COL2A1 were dropped respectively (diluted at 1:100). The wet box was incubated at 4°C overnight. The excess primary antibodies were removed and washed three times with PBS for 10 minutes each time. Add the secondary antibody dropwise (diluted at 1:100) and incubate at room temperature in the dark for 1-2hours. After removing the secondary antibody, wash with PBS. After scanning the sectioning instrument, 10 fields of view were randomly selected to calculate their fluorescence IOD values and the AREA of the entire field of view map of AREA using IPP. Mean optical density (MOD) = IOD/AREA. The specific parameters of each antibody are as follows in Table 3.

Table 3: Information related to the antibodies used in the IF experiment

Antibody name	Cat#	Lot	Host species
IL-1β	A11370	0204210301	Rabbit
MMP-7	A0695	3517037101	Rabbit
LOXL2	A14638	5500007349	Rabbit
COL2A1	A19308	3561189105	Rabbit

Note: All antibodies in this table are rabbit-derived polyclonal antibodies, purchased from Abclonal Technology Co., Ltd. (Wuhan, China).

ELISA: Metatarsophalangeal articular cartilage-subchondral bone tissues were excised, weighed, and liquid nitrogen-homogenized. Homogenates were centrifuged at 3,000rpm for 15min, and supernatants were collected. Protein concentrations in supernatants were quantified, and target protein levels were normalized to total protein content (ng/g) for subsequent analysis. For ELISA, protein levels of IL-1β, MMP-7, LOXL2, and COL2 were measured using kits from Jiangsu Enzyme Immunoassay Industry Co., LOD (<1.0pg/mL). Briefly, supernatants and serially diluted standards were added to pre-coated wells and incubated at 37°C for 60 minutes. After incubation, wells were washed five times with wash buffer to remove unbound components. Then, HRP-conjugated detection antibodies were added, followed by another 30-minute incubation at 37°C. Subsequently, wells were washed again, and substrate solution was added for color development in the dark at 37°C for 15minutes. The reaction was terminated with stop solution, and absorbance was read at 450nm (OD). Sample concentrations were calculated via linear regression, using the standard curve generated from OD values and known concentrations of standards. Finally, inter-group differences in inflammatory factor expression were analyzed by one-way ANOVA combined with Tukey's multiple comparison test.

Statistical analysis: All statistical analyses were performed using GraphPad Prism 9.5.0 (GraphPad Software, San Diego, CA, USA). Prior to analysis, data normality was verified using the Shapiro-Wilk test. All data are presented as mean±standard error of the mean (SEM). Differences between the three groups (H, D1, D2) were analyzed by one-way analysis of variance (ANOVA), followed by Tukey's multiple comparison test for post-hoc pairwise comparisons. Statistical significance is defined as follows: $P<0.05$ indicates a significant difference, while $P<0.01$ indicates an extremely significant difference.

RESULTS

General observation: Ostriches exhibiting normal feed and water intake, normal spirit, and no behavioral abnormalities were assigned to the H group. Those with metatarsophalangeal joint swelling and mild lameness were assigned to the D1 group, while ostriches with metatarsophalangeal joint swelling, severe locomotor impairment, and recumbency were assigned to the D2 group (Fig. 1).

Joint fluid volume and circumference measurements: Compared with the H group (joint fluid volume: 3.32±0.68mL; joint circumference: 12.51±1.20cm), both D1 groups (joint fluid volume: 6.05±0.83mL; joint circumference: 15.67±1.11cm) and D2 groups (joint fluid volume: 8.38±1.42mL; joint circumference: 16.93±1.06cm) exhibited an extremely significant increase in synovial fluid volume ($P<0.01$), with the D2 group significantly higher than D1 ($P<0.01$). Likewise, joint circumference was extremely significantly increased in both D groups versus H ($P<0.01$), and significantly greater in D2 than D1 ($P<0.05$) (Fig. 2).

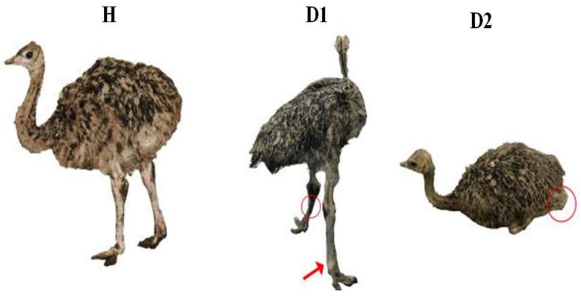

Fig. 1: Morphological changes in the joints of affected ostrich compared to control. Note: H: Healthy ostriches; D1: Ostriches with mild disease (Ostriches with swollen metatarsophalangeal joints and lameness). D2: Ostriches with severe disease (Ostriches with swollen joints, difficulty in moving, and being unable to stand.) Circle : limp; →: Joint swelling.

Pathological changes in cartilage and subchondral bone: To elucidate the effects of ostriches with leg and toe disease on cartilage and subchondral bone, tissues were examined from the surface inward. Superficial zone (Fig. 3A): In H ostriches, the cartilage surface was intact, with dense, well-aligned collagen fibers and abundant chondrocytes. In D1 ostriches, the surface appeared rough, chondrocyte numbers decreased, collagen fibers were fragmented, and inter-fiber gaps widened. In D2 ostriches, chondrocyte loss was extensive and collagen fiber architecture was severely disrupted, with large defects. Middle zone (Fig. 3B, E-F): In the H group, chondrocytes were abundant and evenly distributed. In D1 and D2 groups, focal chondrocyte necrosis and a marked increase in empty cartilage lacuna were observed, worsening with lesion severity. Quantification showed a highly significant decrease in chondrocyte count (E: by ~40% in D1 vs H, $P<0.01$; a ~43% in D2 vs D1, $P<0.01$) and a highly significant increase in empty lacuna rate (F: by ~30% in D1 vs H, $P<0.01$; by ~43% in D2 vs D1, $P<0.01$) in D groups as compared to H. Subchondral bone (Fig. 3C, G–I): H ostriches displayed a clear trabecular structure. In D groups, trabecular thickness decreased (G: by ~33% in D1 vs H, $P<0.01$; by ~37% in D2 vs D1, $P<0.01$) and trabecular spacing was markedly altered (H: by ~40% in D1 vs H, $P<0.01$; by ~33% in D2 vs D1, $P<0.01$). Osteoblast counts in the subchondral region increased highly significantly with disease progression (I: by ~45% in D1 vs H, $P<0.05$; by ~90% in D2 vs H, $P<0.01$). These findings indicate that ostrich leg and toe disease primarily induced structural alterations in the outer cartilage, characterized by significant chondrocyte loss, and localized bone formation in the subchondral region.

Since ECM was the survival niche for chondrocytes and facilitates material exchange with them, the reduction in chondrocytes in group D led to decreased ECM content. To assess this, we used Masson staining to examine changes in collagen-a major component of the ECM. In group H, ECM stained blue and collagen fibers appeared red, with clear, intact architecture. Compared to the H group, cartilage matrix and collagen fiber staining in D groups were fainter, collagen protein was significantly reduced, and the outer cartilage layer showed collagen fiber defects. Relative to group D1, staining in the group D2 was even fainter, collagen protein was further reduced, and outer-layer collagen fiber defects were more severe (Fig. 4.).

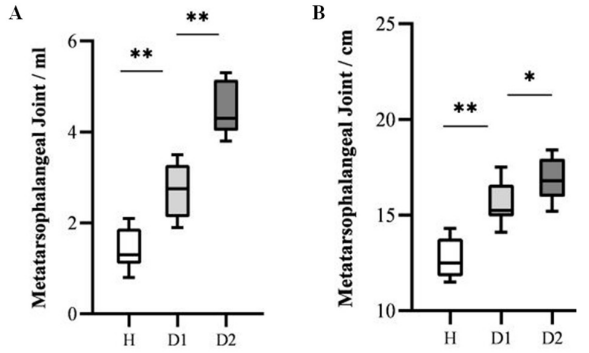

Fig. 2: Comparison of joint fluid volume (A) and joint circumference (B) among healthy and diseased ostriches H: Healthy ostriches; D1: Ostriches with mild disease; D2: Ostriches with severe disease. A: Comparison of total amount of joint fluid; B: Comparison of joint circumference. Note: A: The comparison of the total amount of joint fluid showed that its content increased as the degree of lesion worsened. B: The comparison of joint circumference shows that its joint circumference increases as the severity of the lesion worsens. (Statistical significance is denoted by *$P<0.05$, **$P<0.01$).

Validation of disease severity: Based on results before, Mankin's scoring of HE-stained cartilage revealed that D1 scores were significantly higher than H ($P<0.01$), and D2 scores were significantly higher than D1 ($P<0.01$) (Fig. 5.). This confirms that clinical grouping corresponds to actual cartilage pathology, validating the H, D1, and D2 classifications. Expression of key lnflammatory mediators in cartilage–subchondral bone

qRT-PCR of mRNA expression: mRNA expression levels were quantified using qRT-PCR, with GAPDH as the internal reference gene and relative expression calculated via the $2^{(-\Delta\Delta Ct)}$ method. IL-1β mRNA in D1 was significantly elevated versus H (4.56±1.34-fold, $P<0.05$), and further highly elevated in D2 versus D1 (8.23±2.09-fold vs. H, $P<0.01$). LOXL2 mRNA in D1 was significantly reduced versus H (0.62±0.31-fold, $P<0.05$), with further reduction in D2 versus D1 (0.46±0.08-fold vs. H, $P<0.05$). MMP-7 mRNA in both D1 and D2 was extremely significantly higher than H (D1: 4.06±1.60-fold, $P<0.01$; D2: 5.70±4.34-fold, $P<0.01$), with D2 exceeding D1 ($P<0.01$). COL2A1 mRNA in D1 was extremely significantly lower than H (0.45±0.05-fold, $P<0.01$) and further reduced in D2 versus D1 (0.16±0.02-fold vs. H, $P<0.01$). The above findings indicate that the disease course of ostrich toe and leg disease is affected by the expressions of IL-1β, MMP-7, LOXL2 and COL2A1 (Fig. 6.).

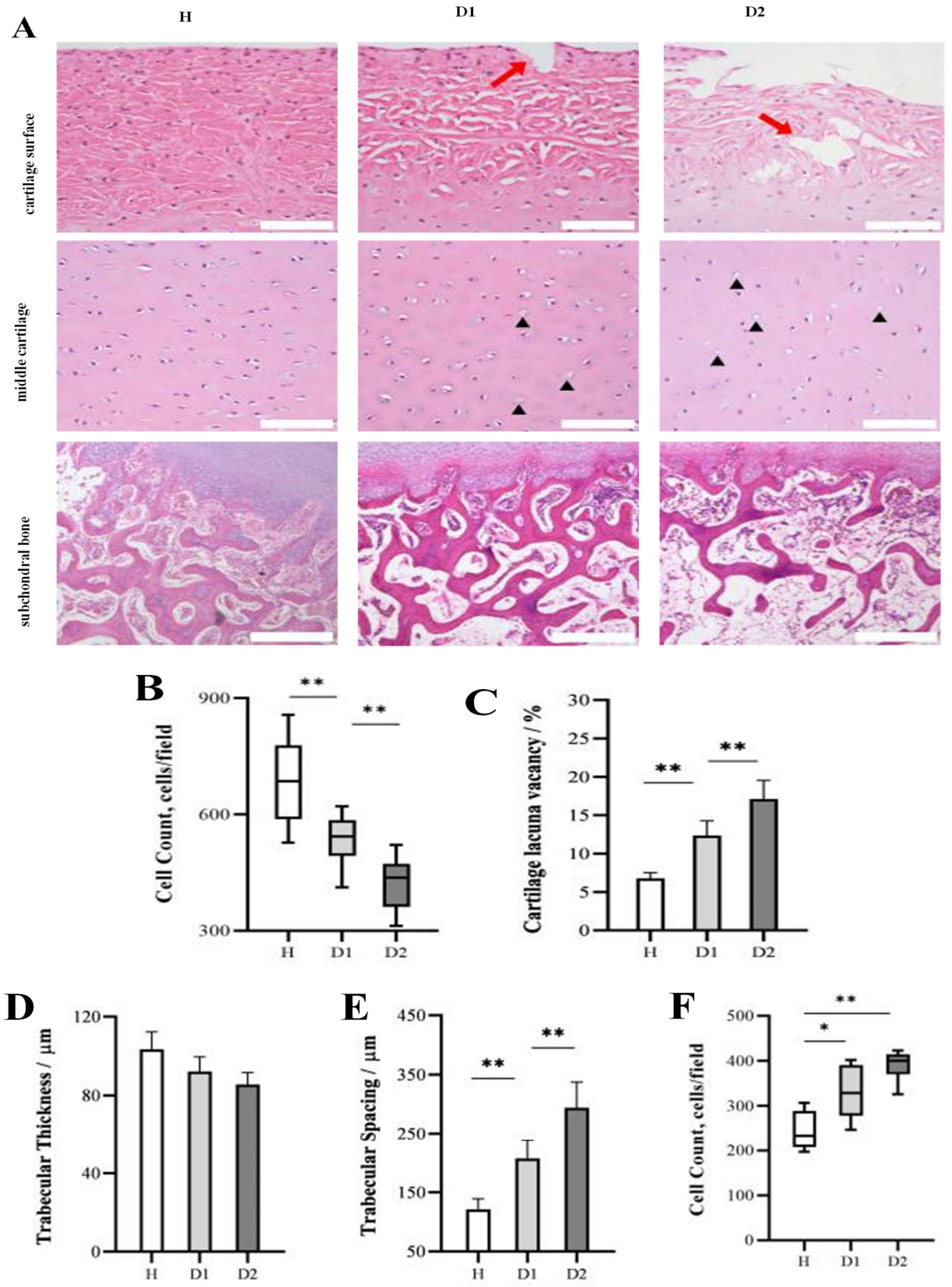

Fig. 3: Pathological changes and microscopic quantitative analysis results of metatarsophalangeal joint cartilage and subchondral bone. H: Healthy ostriches; D1: Ostriches with mild disease; D2: Ostriches with severe disease. A: Pathological changes of metatarsophalangeal articular cartilage and subchondral bone. →: the outer membrane of the cartilage is damaged, ▲: cartilaginous lacuna empty. (H&E, magnification 400, 400, and 40×, scale bar = 50, 50, 100μm). B: Chondrocyte count; C: Cartilage, acuna vacancy rate; D: Bone trabecular thickness; E: Trabecular spacing; F: Osteoblast count. It indicates that as the severity of the lesion increases, it mainly causes damage to the outer layer of the joint cartilage and a significant reduction in the number of cartilage cells within it. (Statistical significance is denoted by *P<0.05, **P<0.01.)

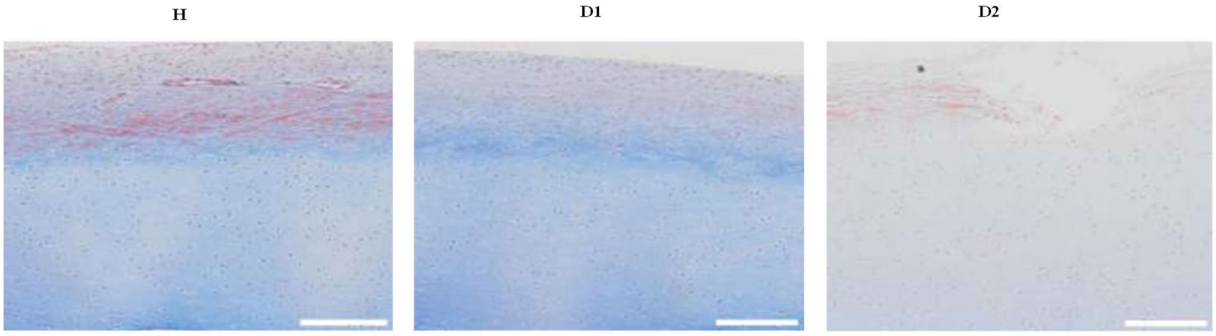

Fig. 4: Masson staining results of metatarsophalangeal articular cartilage. H: Healthy ostriches; D1: Ostriches with mild disease; D2: Ostriches with severe disease. It shows that as the severity of the lesion increases, the degradation of the ECM of chondrocytes and the rupture of collagen fibers on the cartilage surface become more severe. →: defects of the outer cartilage membrane space and collagen fibers. (Masson staining, the magnification is 200×, scale bar =20μm).

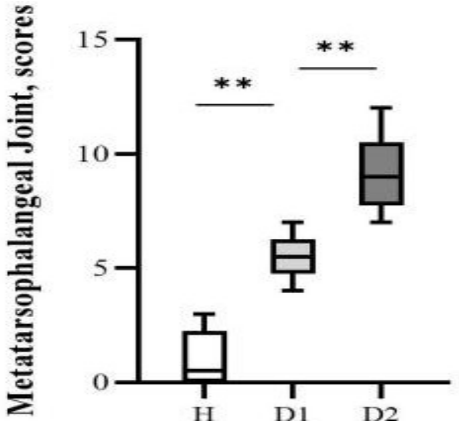

Fig. 5: Metatarsophalangeal joint lesion degree score. H: Healthy ostriches; D1: Ostriches with mild disease; D2: Ostriches with severe disease. This indicates that the results of this experiment in determining the degree of disease in ostriches are reasonable. Data are lower limit, lower quartile, median, upper quartile and upper limit (n=6; statistical significance is denoted by *P<0.05, **P<0.01).

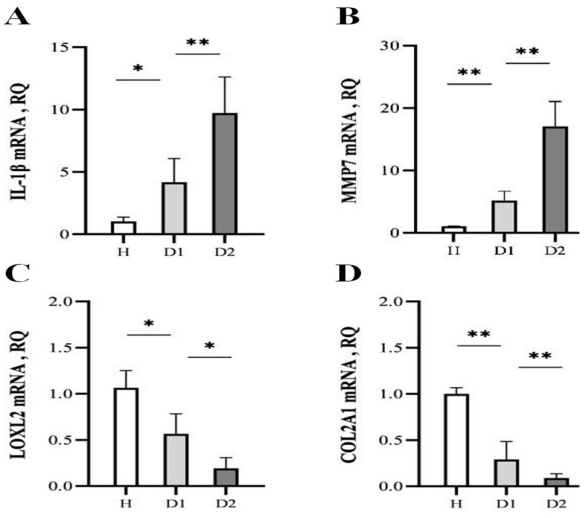

Fig. 6: The relative expression levels of mRNA of IL-1β/MMP-7/LOXL2/COL2A1 in ostriches with toe and leg disease. H: Healthy ostriches; D1: Ostriches with mild disease; D2: Ostriches with severe disease. A: Relative expression of IL-1β mRNA; B: Relative expression of MMP-7 mRNA; C: Relative expression of LOXL2 mRNA; D: Relative expression of COL2A1 mRNA. This indicates that the mRNA of those four factors is related to the severity of the lesion. (Statistical significance is denoted by *P<0.05, **P<0.01).

IF localization and expression: To localize and quantify protein expression, IF was performed (Fig. 7.). IL-1β (Fig. 7A-D): Expression in the middle layer of articular cartilage in articular cartilage, and mainly on osteoblasts, osteoclasts and osteocytes in subchondral bone. Fluorescence intensity was significantly greater in D1 versus H (P<0.01) and further increased in D2 versus D1 (P<0.01), mirroring mRNA trends. MMP-7 (Fig. 7E-H): Expression exhibited nuclear localization in all detected regions, was in the middle layer of articular cartilage, and mainly on the nuclei of osteocytes in subchondral bone. Expression was significantly greater in D1 versus H (P<0.01) and further increased in D2 versus D1 (P<0.01), consistent with mRNA findings. LOXL2 (Fig. 7I-L): Expression showed nuclear localization in all detected regions, was in the middle layer of articular cartilage, and mainly on the nuclei of osteocytes in subchondral bone. Expression was highly significantly reduced in D1 versus H (P<0.01) and further reduced in D2 versus D1 (P<0.01), consistent with transcript data. COL2A1 (Fig. 7M-P): Mainly distributed in the middle layer of articular cartilage in articular cartilage and mainly exists in the bone matrix in subchondral bone. Expression was significantly decreased in D1 versus H (P<0.01) and further decreased in D2 versus D1 (P<0.01), matching mRNA findings.

ELISA of protein concentration: To further verify the protein expression levels of key inflammatory factors, ELISA was used to verify the protein expression levels of key inflammatory factors in the metatarsophalangeal articular cartilage-subchondral bone tissue homogenate, with protein concentrations normalized to total protein content (ng/mg total protein). ELISA quantification in tissue homogenates (Fig. 8.) showed: IL-1β and MMP-7 protein levels were highly significantly increased in D1 versus H (IL-1β: H: 3.85±1.16ng/mg, D1: 5.21±1.28ng/mg, P<0.01; MMP-7: H: 2.35±0.85ng/mg, D1: 5.33±1.14ng/mg, P<0.01) and further in D2 versus D1 (IL-1β: 8.59±1.11ng/mg, P<0.01; MMP-7: 9.20±1.85ng/mg, P<0.01). LOXL2 protein was highly significantly decreased in D1 versus H (H: 5.34±1.36ng/mg, D1: 3.44±1.05ng/mg, P<0.01) and further in D2 versus D1 (2.22±1.45ng/mg, P<0.01). COL2 protein was highly significantly decreased in D1 versus H (H: 28.24±1.21, D1: 19.96±1.18ng/mg, P<0.01) and significantly lower in D2 versus D1 (15.02±1.16ng/mg, P<0.05). These ELISA findings corroborate the qRT-PCR and IF findings, confirming that IL-1β, MMP-7, LOXL2, and COL2A1 are integrally involved in the pathogenesis of Ostrich leg and toe disease.

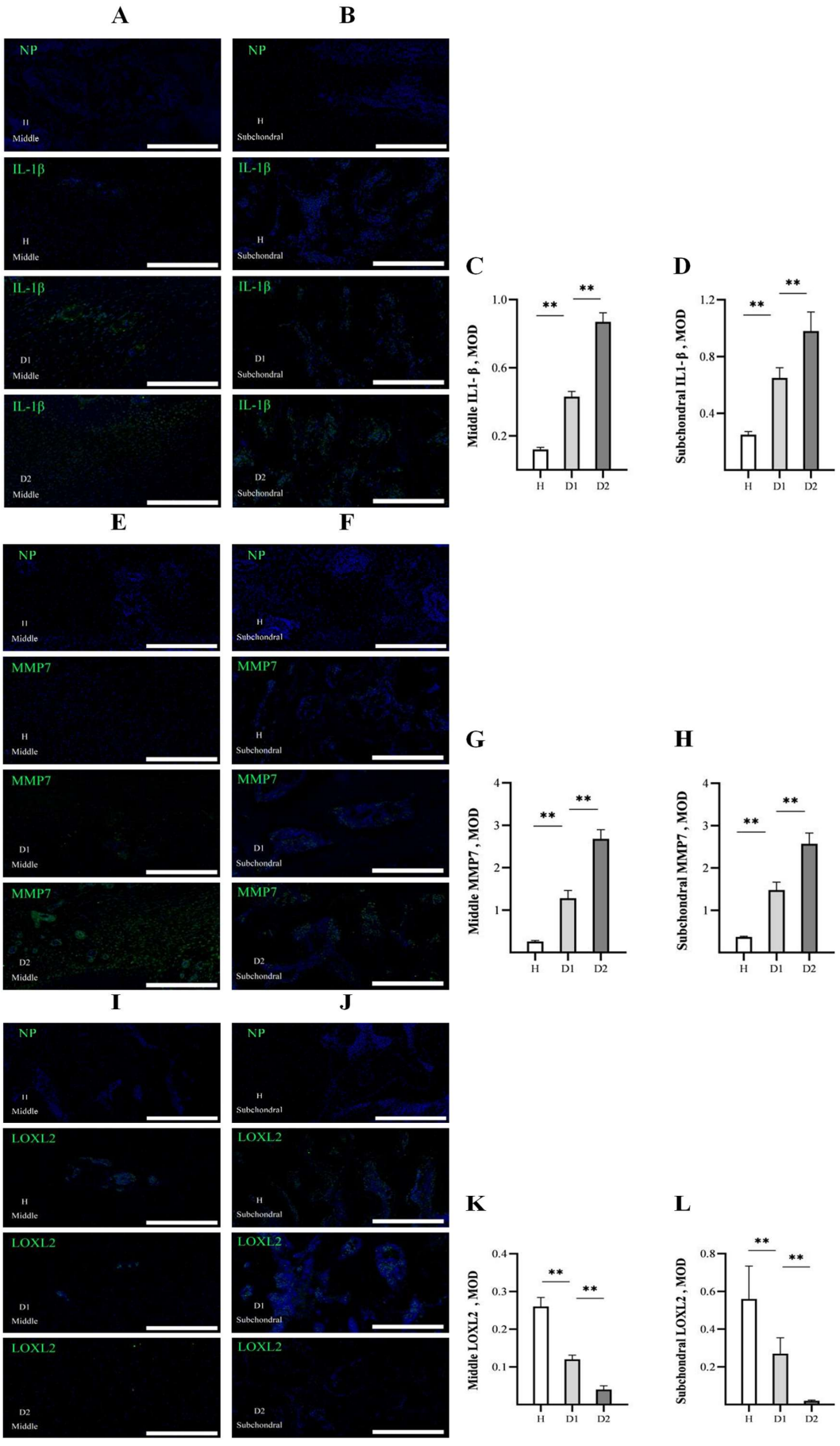
A
B
NP
H
Middle
Subchondral
IL-1β
D1
D2
C
D
Middle IL1-β, MOD
Subchondral IL1-β, MOD
**
H
D1
D2
E
F
MMP7
G
H
Middle MMP7, MOD
Subchondral MMP7, MOD
I
J
LOXL2
K
L
Middle LOXL2, MOD
Subchondral LOXL2, MOD

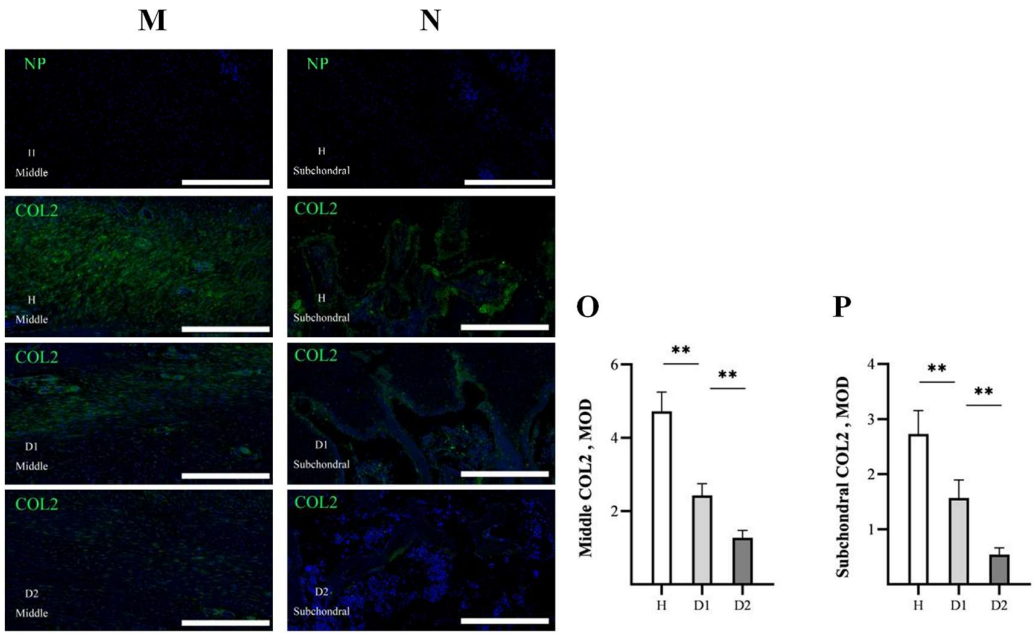

Fig. 7: Localization and expression in cartilage and subchondral bone of IL-1β/MMP-7/LOXL2/COL2 by IF. Note: NP: No primary. H: Healthy ostriches; D1: Ostriches with mild disease; D2: Ostriches with severe disease. A: IL-1β in the middle layer of cartilage; B: IL-1β in the subchondral bone; C: IL-1β in the middle layer of cartilage MOD value of; D: IL-1β in the subchondral bone MOD value of. Panels A-D show that as the severity of the lesion increases, the expression level of IL-1β also rises. E: MMP-7 in the middle layer of cartilage; F: MMP-7 in the subchondral bone; G: MMP-7 in the middle layer of cartilage MOD value of; H: Subchondral bone MOD value of MMP-7. Panels E-H indicate that as the severity of the lesion increases, the expression level of MMP-7 rises. I: LOXL2 in the middle layer of cartilage; J: LOXL2 in the subchondral bone; K: LOXL2 in the middle layer of cartilage MOD value of; L: Subchondral bone MOD value of LOXL2. Panels I-L show that as the severity of the lesion increases, the expression level of LOXL2 decreases. M: COL2 in the middle layer of cartilage; N: COL2 in the subchondral bone; O: COL2 in the middle layer of cartilage MOD value of; P: Subchondral bone MOD value of COL2. Panels M-P indicate that: as the severity of the lesion increases, the expression level of COL2 also decreases. (IF, the magnification is 200×, scale bar =100μm. Statistical significance is denoted by *P<0.05, **P<0.01.)

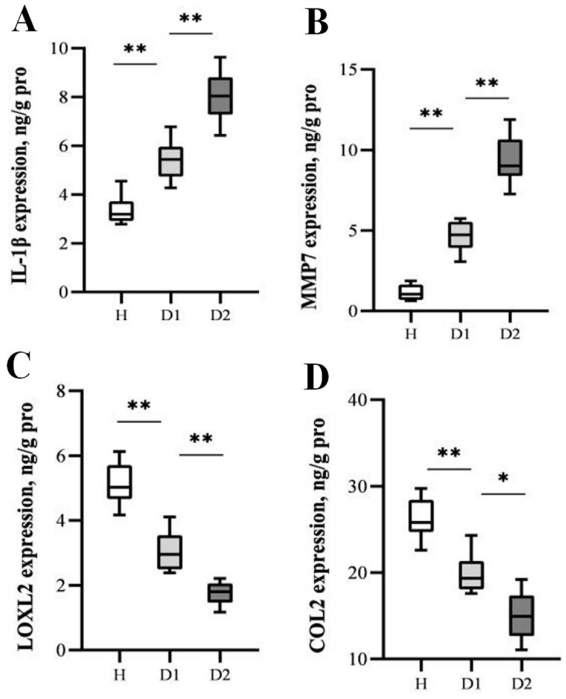

Fig. 8: The expression of IL-1β/MMP-7/LOXL2/COL2 in ostriches with toe and leg diseases was determined by ELISA. Note: H: Healthy ostriches; D1: Ostriches with mild disease; D2: Ostriches with severe disease. A: IL-1β protein expression; B: MMP-7 protein expression; C: LOXL2 protein expression; D: COL2 protein expression. This indicates that the protein contents of these four factors are related to the severity of the lesion. (Statistical significance is denoted by *P<0.05, **P<0.01).

DISCUSSION

The main pathological changes of ostrich leg and toe disease in cartilage were a significant increase in necrotic chondrocytes and empty chondrocyte lacunae, along with decreased ECM. In subchondral bone, the key alterations included an increased number of osteoblasts and widened trabecular bone spacing.

Based on these findings, we speculate that the pathological process of ostrich toe leg disease may be initiated by intra-articular cytokine alterations. These changes subsequently lead to chondrocyte loss and ECM reduction. As the ECM degrades, its degradation products further stimulate chondrocytes to secrete related inflammatory factors (Xu *et al*., 2021). This stimulation promotes synovial fluid production in the synovium. The compensatory increase in synovial fluid induces metatarsophalangeal joint swelling and increased joint circumference. Moreover, collagen network integrity and proteoglycan synthesis/storage determine the physical properties of the cartilage tissue structure. Disruption of this metabolic balance leads to loss of elastic components in the collagen network. This results in reduced cartilage hardness and elasticity (Li and Wu, 2021). Chondrocytes are subjected to dual stressors: mechanical stress and an altered microenvironment (i.e., ECM degradation). This disrupts their normal metabolic balance, causing extensive chondrocyte necrosis. After chondrocyte necrosis, surrounding ECM fails to fill the vacated lacunae. This leads to the formation of numerous empty chondrocyte lacunae (Im and Kim, 2014). Additionally, cartilage and

subchondral bone exhibit mutual pressure transmission and release effects. Disruption of normal cartilage structure increases mechanical stress transmitted to the subchondral bone. When this stress exceeds the adaptive capacity of the cartilage-subchondral bone unit, it triggers local bone formation and regulates subchondral bone remodeling. This leads to trabecular spatial structure alterations and widened trabecular spacing (Li *et al*., 2013). To compensate for the increased pressure, subchondral bone exhibits a significant increase in osteoblast numbers, which enhances local bone density. This irreversible process severely affects the normal activity of the affected limp (Zheng *et al*., 2021)

Studies have shown that IL-1β is a major proinflammatory cytokine in OA (Li *et al*., 2021) stimulating the occurrence and development of inflammatory responses in articular cartilage, which is analogous to its role in mammalian OA. Moreover, IL-1β can promote the production of catabolic factors (e.g., MMPs) and inhibits anabolic activity, down-regulating ECM components like COL2A1 (Chadjichristos *et al*., 2003; Shakibaei *et al*., 2005; Weber *et al*., 2021). In OA, the expression levels of IL-1β in synovial fluid, synovium, subchondral bone, and cartilage are significantly increased (Fei *et al*., 2019). In this study, elevated IL-1β in diseased metatarsophalangeal joints correlated with reduced COL2A1, ECM breakdown, and superficial collagen fiber rupture-supporting its role as a key initiator of ostrich leg and toe disease.

In addition, IL-1β can stimulate chondrocytes to release several proteolytic enzymes, including MMPs: MMP-1, MMP-3, MMP-7, and MMP-13 (Mengshol *et al*., 2000) which drive cartilage ECM breakdown via nuclear factor-mediated transcriptional activation of pro-collagenases (Galis and Khatri, 2002). While MMP-1 and MMP-13 are well-characterized in joint pathology (Kapoor *et al*., 2011), our finding of markedly increased MMP-7 in diseased ostrich joints suggested it may be a species-specific mediator. Future studies should validate MMP-7's enzymatic cleavage targets in avian cartilage ECM to confirm its functional role, which could inform disease-specific diagnostics.

In contrast, LOXL2 exerts protective effects on articular cartilage by mitigating mechanical stress-induced damage, enhancing COL2 and proteoglycan expression, and attenuating pro-inflammatory signaling (Ferreira *et al*., 2021; Miao *et al*., 2024). In this study, decreased LOXL2 expression in diseased joints aligns with progressive cartilage degeneration of leg and toe disease implying that enhancing LOXL2 activity may represent a potential target for addressing ostrich leg and toe disease. These findings suggest that appropriately increasing the expression of LOXL2 may help alleviate disease progression.

Conclusions: Ostrich leg and toe disease features increased IL-1β and MMP-7 with decreased LOXL2 and COL2A1 across disease severities, paralleling progressive cartilage-subchondral bone pathology and highlighting these mediators as mechanistic and potential diagnostic targets.

Authors contribution: Conceptualization: LT, BWD; Methodology: LT, BWD; Investigation: LT, BWD (performed the experiments); BWD (collected the samples); Formal analysis: BWD (including statistical analysis of experimental results); Writing-original draft: YYD, BWD; Writing-review & editing: All authors; Final approval: All authors.

Acknowledgements: All animal-related procedures were conducted in accordance with the Animal Care and Use Committee of Sichuan Agricultural University (SYXK 2019-187). The authors are thankful to the Sanmu ostrich breeding farm in Mianyang city.

REFERENCES

Alshenibr W, Tashkandi MM, Alsaqer SF, *et al*., 2017. Anabolic role of lysyl oxidase like-2 in OA cartilage. Arthritis Research and Therapy 19:38.

Arend WP, Palmer G and Gabay C, 2008. IL-1, IL-18, and IL-33 families of cytokines. Immunological Reviews 223:20-38.

Bowen D, 2023. Pathomorphological and expression of related gene of metatarsophalangeal joint and subchondral in ostrich with toe and leg disease. Sichuan Agricultural University.

Chadjichristos C, Ghayor C, Kypriotou M, *et al*., 2003. Sp1 and Sp3 transcription factors mediate interleukin-1 beta down-regulation of human type II collagen gene expression in articular chondrocytes. Journal of Biological Chemistry 278:39762-39772.

Cheng JH, Chou WY, Wang CJ, *et al*., 2022. Pathological, morphometric and correlation analysis of the modified Mankin score, tidemark roughness and calcified cartilage thickness in rat knee osteoarthritis after extracorporeal shockwave therapy. International Journal of Medical Sciences 19:242-256.

Chiba K, Uetani M, Kido Y, *et al*., 2012. Osteoporotic changes of subchondral trabecular bone in osteoarthritis of the knee: a 3-T MRI study. Osteoporosis International 23:589-597.

Deng B, Wang F, Yin L, *et al*., 2016. Quantitative study on morphology of calcified cartilage zone in OARSI 0–4 cartilage from osteoarthritic knees. Current Research in Translational Medicine 64:149-154.

Fei J, Liang B, Jiang C, *et al*., 2019. Luteolin inhibits IL-1β-induced inflammation in rat chondrocytes and attenuates osteoarthritis in a rat model. Biomedicine and Pharmacotherapy119: 1586-1592.

Ferreira S, Saraiva N, Rijo P, *et al*., 2021. LOXL2 inhibitors and breast cancer progression. Antioxidants 10:312.

Galis ZS and Khatri JJ, 2002. Matrix metalloproteinases in vascular remodeling and atherogenesis: the good, the bad, and the ugly. Circulation Research 90:251-262.

Goldring SR and Goldring MB, 2016. Changes in the osteochondral unit during osteoarthritis: structure, function and cartilage-bone crosstalk. Nature Reviews Rheumatology 12:632-644.

Hamann N, Zaucke F, Dayakli M, *et al*., 2013. Growth-related structural, biochemical, and mechanical properties of the functional bone-cartilage unit. Journal of Anatomy 222:248-259.

Im GI and Kim MK, 2014. The relationship between osteoarthritis and osteoporosis. Journal of Bone and Mineral Metabolism 32:101-109.

Kapoor M, Martel-Pelletier J, Lajeunesse D, *et al*., 2011. Role of proinflammatory cytokines in the pathophysiology of osteoarthritis. Nature Reviews Rheumatology 7:33-42.

Li G, Yin J, Gao J, *et al*., 2013. Subchondral bone in osteoarthritis: insight into risk factors and microstructural changes. Arthritis Research and Therapy 15:223.

Li SH and Wu QF, 2021. MicroRNAs target on cartilage extracellular matrix degradation of knee osteoarthritis. European Review for Medical and Pharmacological Sciences 25:1185-1197.

Li S, Stöckl S, Lukas C, *et al*., 2021. Curcumin-primed human BMSC-derived extracellular vesicles reverse IL-1β-induced catabolic responses of OA chondrocytes by upregulating miR-126-3p. Stem Cell Research and Therapy 12:252.

Liu Z and Tang X, 2001. Diagnosis and treatment of leg disease in young ostriches. Hunan Journal of Animal Science and Veterinary Medicine 2:2.

Lohmander LS, Hellot S, Dreher D, *et al*., 2014. Intraarticular sprifermin (recombinant human fibroblast growth factor 18) in knee osteoarthritis: a randomized, double-blind, placebo-controlled trial. Arthritis and Rheumatology 66:1820-1831.

Lories RJ and Luyten FP, 2011. The bone-cartilage unit in osteoarthritis. Nature Reviews Rheumatology 7:43-49.

Mao Y, Block T, Singh-Varma A, *et al.*, 2019. Extracellular matrix derived from chondrocytes promotes rapid expansion of human primary chondrocytes in vitro with reduced dedifferentiation. Acta Biomaterialia 85:75-83.

Mengshol JA, Vincenti MP, Coon CI, *et al.*, 2000. Interleukin-1 induction of collagenase-3 (matrix metalloproteinase-13) gene expression in chondrocytes requires p38, c-Jun N-terminal kinase, and nuclear factor kappaB. Arthritis and Rheumatism 43:801-811.

Miao X, Duan B, Tang L, *et al.*, 2024. Chondrocyte apoptosis as a potential mechanism in ostrich limb and toe disorders: a pathological investigation. Pakistan Veterinary Journal 44:71-78.

Mushi EZ, Binta MG, Chabo RG. 2023. Limb deformities of farmed ostrich (Struthio camelus) chicks in Botswana. Tropical Animal Health and Production 55:412.

Neuhold LA, Killar L, Zhao W, *et al.*, 2001. Postnatal expression in hyaline cartilage of constitutively active human collagenase-3 (MMP-13) induces osteoarthritis in mice. Journal of Clinical Investigation 107:35-44.

Park NR, Lim KE, Han MS, *et al.*, 2016. Core binding factor β plays a critical role during chondrocyte differentiation. Journal of Cellular Physiology 231:162-171.

Peel MJ, Torres RSG, Ivančić M, *et al.*, 2022. Management of intertarsal septic arthritis in an ostrich (Struthio camelus). Veterinary Medicine and Science 8:125-129.

Reina N, Cavaignac E, Pailhé R, *et al.*, 2017. BMI-related microstructural changes in the tibial subchondral trabecular bone of patients with knee osteoarthritis. Journal of Orthopaedic Research 35:1653-1660.

Roy S, Khanna S, Krishnaraju AV, *et al.*, 2006. Regulation of vascular responses to inflammation: inducible matrix metalloproteinase-3 expression in human microvascular endothelial cells is sensitive to anti-inflammatory Boswellia. Antioxidants and Redox Signaling 8:653-660.

Sengupta K, Kolla JN, Krishnaraju AV, *et al.*, 2011. Cellular and molecular mechanisms of anti-inflammatory effect of Aflapin: a novel Boswellia serrata extract. Molecular and Cellular Biochemistry 354:189-197.

Shakibaei M, Schulze-Tanzil G, John T, *et al.*, 2005. Curcumin protects human chondrocytes from IL-1β-induced inhibition of collagen type II and β1-integrin expression and activation of caspase-3. Annals of Anatomy 187:487-497.

Tang L, Zhang Y and Peng K, 2012. Discussion on the causes and comprehensive preventive measures of toe and leg diseases in young ostriches. Progress in Veterinary Medicine 05:131-134.

Umar Z, 2021. Macroscopic, microscopic and histomorphometric analysis of intestine, liver and pancreas of ostrich (Struthio camelus) with advancement of age and sex. Pakistan Veterinary Journal 41:313-320.

Weber AE, Bolia IK and Trasolini NA, 2021. Biological strategies for osteoarthritis: from early diagnosis to treatment. International Orthopaedics 45:335-344.

Xu Z, Ke T, Zhang Y, *et al.*, 2021. Danshensu inhibits the IL-1β-induced inflammatory response in chondrocytes and osteoarthritis possibly via suppressing NF-κB signaling pathway. Molecular Medicine 27:80.

Yuan K, Wang D, Luan Q, *et al.*, 2020. Whole genome characterization and genetic evolution analysis of a new ostrich parvovirus. Viruses 12:334.

Zheng L, Zhang Z, Sheng P, *et al.*, 2021. The role of metabolism in chondrocyte dysfunction and the progression of osteoarthritis. Ageing Research Reviews 66:101249.

Zhou Y, Wang L and Zhou F, 2023. Clinical significance of MMP7 levels in colorectal cancer patients receiving FOLFOX4 chemotherapy treatment. International Journal of General Medicine 16:2671-2678